



Fermi National Accelerator Laboratory

FERMILAB-FN-631

CMS Hadronic Calorimetry Simulation Using Hanging File Data

I. Gaines, D. Green, J. Marraffino, J. Womersley and W. Wu

*Fermi National Accelerator Laboratory
P.O. Box 500, Batavia, Illinois 60510*

S. Kunori

*University of Maryland
College Park, Maryland 20742*

May 1995

Disclaimer

This report was prepared as an account of work sponsored by an agency of the United States Government. Neither the United States Government nor any agency thereof, nor any of their employees, makes any warranty, expressed or implied, or assumes any legal liability or responsibility for the accuracy, completeness, or usefulness of any information, apparatus, product, or process disclosed, or represents that its use would not infringe privately owned rights. Reference herein to any specific commercial product, process, or service by trade name, trademark, manufacturer, or otherwise, does not necessarily constitute or imply its endorsement, recommendation, or favoring by the United States Government or any agency thereof. The views and opinions of authors expressed herein do not necessarily state or reflect those of the United States Government or any agency thereof.

Fermilab-FN-631

April 28, 1995

CMS Hadronic Calorimetry Simulation Using Hanging File Data

I. GAINES, D. GREEN, J. MARRAFFINO, J. WOMERSLEY, W. WU

Fermi National Accelerator Laboratory

P. O. Box 500, Batavia, IL 60510

and

S. KUNORI

University of Maryland

College Park, MD 20742

ABSTRACT

Using recently available data from the Fermilab “hanging file” calorimeter, we have reviewed and extended our previously published study on using weights to improve the resolution of a calorimeter. Since the hanging file calorimeter is substantially more finely segmented than the one used for our earlier study, it is now possible to obtain a much better match to the geometry of the current CMS calorimeter design. In addition, we are able to study some details of the low energy tail of the energy deposition spectrum not previously accessible with the earlier low statistics data sample.

Introduction

We have previously studied how to optimize the CMS hadron calorimetry resolution by assigning weights to certain calorimeter layers¹ using the Fermilab Lab E data set. Due to the coarse sampling thickness and limited number of events, we were not able to parameterize the low energy “tail” induced by leakage nor to match the precise configuration of the CMS hadronic calorimeter. By comparison, the hanging file data set² has very fine sampling thickness compared to the baseline CMS hadron calorimeter, and consists of a large number of events which are available for 25 GeV, 100 GeV and 227 GeV π beams. In this paper, we will focus on the leakage tail parameterization, and re-examine how much benefit will be obtained by having a tail catcher (TC), massless gap (MG) and a weighting strategy.

The Hanging File Data Set

The hanging file data was taken from a reconfigurable-stack calorimeter. The calorimeter stack was formed by a series of 1 m \times 1 m plates. It can be arranged in any combination of layers of scintillator, Pb, Fe, or Al. The technical details can be seen in reference 2. The data set we are using here is Run 1243 with a 227 GeV π beam, Run 1251 with a 100 GeV π beam and Run 1253 with a 25 GeV π beam. For these runs, the configuration is alternating plates of 1 inch Fe and scintillator with a total of 72 layers. With that, we can model the CMS calorimeter as shown in the following table.

Table 1. Hanging File and CMS Configuration

All depths given in units of λ

| | EM | HAC1 | HAC2 | dead | TC |
|--------------------|------|------|------|------|------|
| Hanging file depth | 1.51 | 3.17 | 6.96 | 8.47 | 9.54 |
| CMS design depth | 1.5 | 3.1 | 7.0 | 8.5 | 9.6 |

In the table, EM refers to the $PbWO_4$ crystal electromagnetic calorimeter, HAC1 and HAC2 refer to the two hadron calorimeter compartments, “dead” refers to the inert material of the CMS magnet coil, and TC refers to the so-called tail catcher behind the magnet coil. The CMS configuration is taken from the latest design of the geometry and the materials³ as given in the baseline design report. Following that baseline design, we study the following cases.

- Case A: $|\eta| < 0.7$, with tail catcher and massless gap.
- Case B: $|\eta| > 0.7$, with massless gap but no tail catcher.

Weighting Strategy

The optimum weights were defined to be those which minimize the RMS of energy variation with respect to the energy measured in a calorimeter of depth 10.9λ , and without inert material, and were obtained with a MINUIT program. We found that these weights have only a very weak energy dependence. Thus, we have used the same weights for all beam energies as shown in Table 2. There was no attempt made to use the event by event energy measured in EM, HAC1, HAC2 or TC; the weights are simple constants.

Table 2. Weighting Combination Applied to Various Cases

| Case | Last 2 layers of HAC2 | Massless Gap | Tail Catcher |
|------|-----------------------|--------------|--------------|
| A | 1.5 | 2.5 | 2.0 |
| B | 1.5 | 5.0 | 0.0 |

Note that the weight combinations are not the same for the two cases, since these cases correspond to different calorimeter configurations. Zero means, by definition, there is no tail catcher for case B.

Table 3 shows a summary of results on the Gaussian part of the energy resolution for 25, 100 and 227 GeV beam energy from the CMS hanging file calorimeter. Figures 1, 2 and 3 show the energy distributions for 25, 100 and 227 GeV, with and without weighting and the best (10.9λ) and worst (6.96λ) total depths considered for cases A and B. One can see that the energy resolution is significantly improved by the weighting strategy, and that the massless gap and tail catcher play important roles, especially if we apply an additional weighting. For Case A, we almost reach the performance of the 10.9λ deep calorimeter after applying weighting.

Table 3. Gaussian Energy Resolution (in Percent) With and Without Weighting

| Condition | 25 GeV | 100 GeV | 227 GeV |
|----------------------|--------|---------|---------|
| Case A Unweighted | 12.84 | 7.96 | 6.60 |
| Case A Weighted | 11.97 | 6.93 | 5.27 |
| Case B Unweighted | 13.00 | 8.22 | 6.96 |
| Case B Weighted | 12.13 | 6.99 | 5.44 |
| 10.89 λ cal. | 11.84 | 6.79 | 5.22 |
| 6.96 λ cal. | 13.03 | 8.28 | 7.04 |

Parameterization of the Tail

Due to the limited calorimeter depth, and especially since there is the inert material of the CMS magnet coil in between, we observe a low-side tail, which corresponds to leakage and which degrades the energy resolution. We consider the total energy deposit as consisting of two parts: a Gaussian part in the peak and a non-Gaussian part in the low energy tail. The resolution obtained from the Gaussian part depends on the sampling thickness *etc.*, which we can not do much about. The non-Gaussian part is troublesome for the energy resolution, particularly the missing energy resolution. The weighting strategy is intended to compensate for that problem so that, as a result, the energy resolution, as obtained from the Gaussian part of the data, is improved. Figure 4 shows how the best and the worst energy resolution depends on the energy. The stochastic term, a , defined by $dE/E = a/\sqrt{E} \oplus b$, where \oplus denotes addition in quadrature, varies between 0.571 and 0.589 which is not a significant change, since it depends on mainly the sampling thickness. However the constant term, b , degrades from 0.036 to 0.059, an increase of 63%, due mostly to leakage, which will become more important as the energy increases. All other cases will be located in the

area between of these two lines.

From Figures 1, 2 and 3, we already see clearly the Gaussian part and the tail. In order to make any quantitative statements, it is necessary to first parameterize the shape of the full distribution.

To accomplish that, we proceed as follows. Clearly, the entire energy deposit distribution is dominated by the main Gaussian so that must remain in whatever parameterization we adopt. The form of that Gaussian is given by

$$g(x; A, \mu_1, \sigma_1) = \frac{A}{\sqrt{2\pi\sigma_1^2}} e^{-\frac{(x-\mu_1)^2}{2\pi\sigma_1^2}}.$$

To model the low-energy leakage tail, we add another function made up of two pieces. The first piece is defined as

$$d(x; B, \mu_2, \sigma_2) = \max\left\{0, \frac{d}{dx}g(x; B, \mu_2, \sigma_2)\right\}$$

and is intended to account for the excess data just below the main Gaussian peak without distorting the shape of the spectrum above the main peak. The second piece is intended to account for the long, flat part of the low-energy tail and consists of a simple constant pedestal, K , for $x < \mu_2$ and zero otherwise. In general then, there are 7 parameters in this model. However, it was convenient to impose a constraint among these such that $\mu_2 = \mu_1 - 2\sigma_1$. Otherwise, MINUIT tended to use the functions intended to model the low-energy tail to account for fluctuations in the main peak. This constraint reduced the number of free parameters to six. We also note that the amplitude of each of the three components of our fit is controlled by A , B and K respectively and does not depend on μ or σ . Consequently, the relative strengths of those components can be directly compared.

Figures 5, 6 and 7 show the fitted plots of the full energy spectrum, with and without weighting for Cases A and B at 25, 100 and 227 GeV beam energy. The

tail parameters are summarized in Tables 4, 5 and 6 for the 25, 100 and 227 GeV data respectively. For all of these, the amplitudes A , B and K have been scaled to $A = 1000.0$ to allow direct comparison.

Table 4. Tail Parameterization for the 25 GeV Data

| | 25 GeV $A = 1000.0$ | | | | |
|-------------------|------------------------|------------|--------|------------|--------|
| | μ_1 | σ_1 | B | σ_2 | K |
| Case A Unweighted | 23.9858 | 3.0411 | 4.5194 | 3.2899 | 0.1088 |
| Case A Weighted | 24.5600 | 2.9364 | 0.6605 | 0.0004 | 0.0206 |
| Case B Unweighted | 23.9238 | 3.0681 | 5.5342 | 4.2276 | 0.1655 |
| Case B Weighted | 24.3828 | 2.9546 | 7.6104 | 0.0012 | 0.0444 |

Table 5. Tail Parameterization for the 100 GeV Data

| | 100 GeV $A = 1000.0$ | | | | |
|-------------------|-------------------------|------------|--------|------------|--------|
| | μ_1 | σ_1 | B | σ_2 | K |
| Case A Unweighted | 96.1893 | 7.5029 | 3.9300 | 8.5988 | 0.0302 |
| Case A Weighted | 99.2063 | 6.8672 | 0.0002 | 444.5352 | 0.0182 |
| Case B Unweighted | 95.8540 | 7.6870 | 5.3197 | 9.6973 | 0.0436 |
| Case B Weighted | 98.3420 | 6.8749 | 0.2316 | 0.0314 | 0.0210 |

Table 6. Tail Parameterization for the 227 GeV Data

| | 227 GeV | | | | |
|-------------------|--------------|------------|--------|------------|--------|
| | $A = 1000.0$ | | | | |
| | μ_1 | σ_1 | B | σ_2 | K |
| Case A Unweighted | 222.3673 | 14.4091 | 1.8521 | 16.5039 | 0.0153 |
| Case A Weighted | 229.5469 | 11.9603 | 0.0531 | 27.7715 | 0.0129 |
| Case B Unweighted | 221.4285 | 15.0064 | 2.7796 | 17.4449 | 0.0173 |
| Case B Weighted | 227.4876 | 12.2645 | 0.0000 | 7.2846 | 0.0142 |

One can see that for the same beam energy, the B parameter is much smaller with weight than without weight. That is already apparent from Figures 5, 6 and 7. If we compare the low energy tail between the 10.9λ calorimeter (Figure 8) and the calorimeter after applying the weight (Figures 5, 6 and 7), we find that these tails are essentially the same. This suggests that these events are just ordinary events for which the shower happened to develop very deep in the calorimeter stack. A detailed “scan” of these tail events confirms that supposition. These events represent less than $\approx 1\%$ of the total.

Perhaps, a more interesting comparison is that between our Cases A and B, recalling that the primary difference between them is that Case A includes a tail catcher and Case B does not. We have noted that the parameters used to fit the measured energy deposition distributions vary reasonable smoothly with energy. For some other purposes, we want to apply this tail parameterization at energies other than those where data was taken so we proceed as follows. For any energy other than 25, 100 or 227 GeV, we do a simple linear interpolation between the values shown in Tables 4, 5 and 6 for each of the six parameters needed to fix the distribution. Our first application of this was used to construct Figure 9 which shows the fractional energy resolution as a function of energy for Cases A and B

and includes energies between those where real data was taken. Since the design and use of a tail catcher will generate some new technical problems and increase the overall cost and size of the detector, it is appropriate to try to measure what is gained by including it. The left side of Figure 9 includes the tail catcher while the right side does not. As expected, the tail catcher does improve the fractional resolution but, we note, not by as much as the weighting strategy does. Further test beam data will be taken with copper absorber and an aluminum inert coil mockup in order to confirm this result.

Conclusion

The weighting strategy improves the Gaussian part of the energy resolution at the level of a few percent for 25 GeV, 15 percent for 100 GeV, and as much as 25 percent for 227 GeV, primarily because the tails are much smaller after applying weighting. With the massless gap alone, together with an optimized weighting, we can improve the resolution by an amount which almost but not quite equals that obtained by including a tail catcher.

Acknowledgements

The authors wish to thank Aesook Byon-Wagner and Andy Beretvas who did a very careful hanging file data analysis and for making the data set available for this study.

REFERENCES

1. How to Optimize the CMS Hadron Calorimetry by Assigning Weights to Layers, A. Beretvas, D. Green, J. Marraffino, W. Wu, FNAL-FN-619, May, 1994.
2. Beam Tests of Composite Calorimeter Configurations from a Reconfigurable-stack Calorimeter, A. Beretvas, *et al.*, NIM, A329(1993), 50-61.
3. CMS Technical Proposal, CERN/LHCC 94-38, LHCC/P1, 15 December 1994.

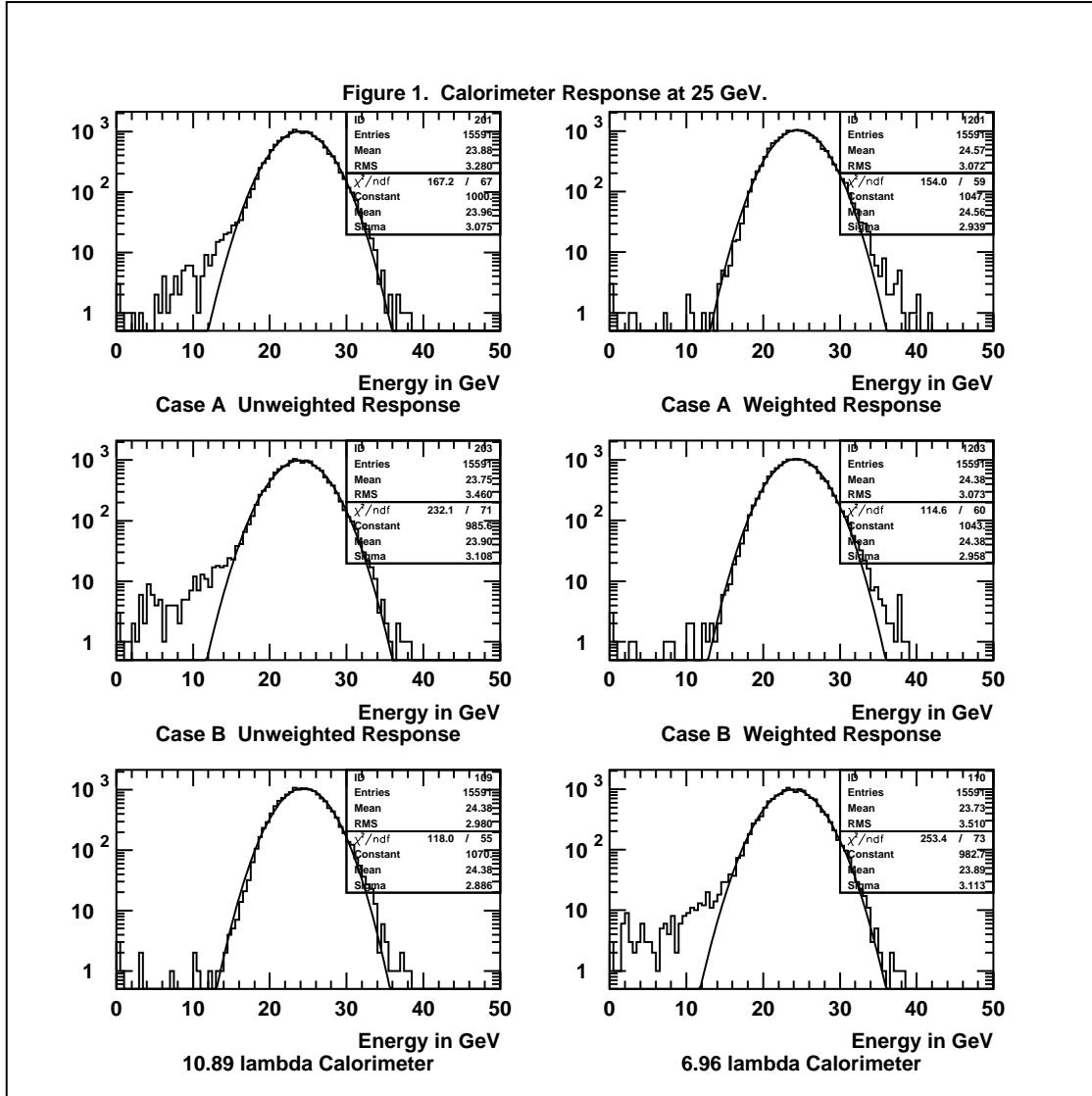


Figure 1. Calorimeter response for a 25 GeV π beam.

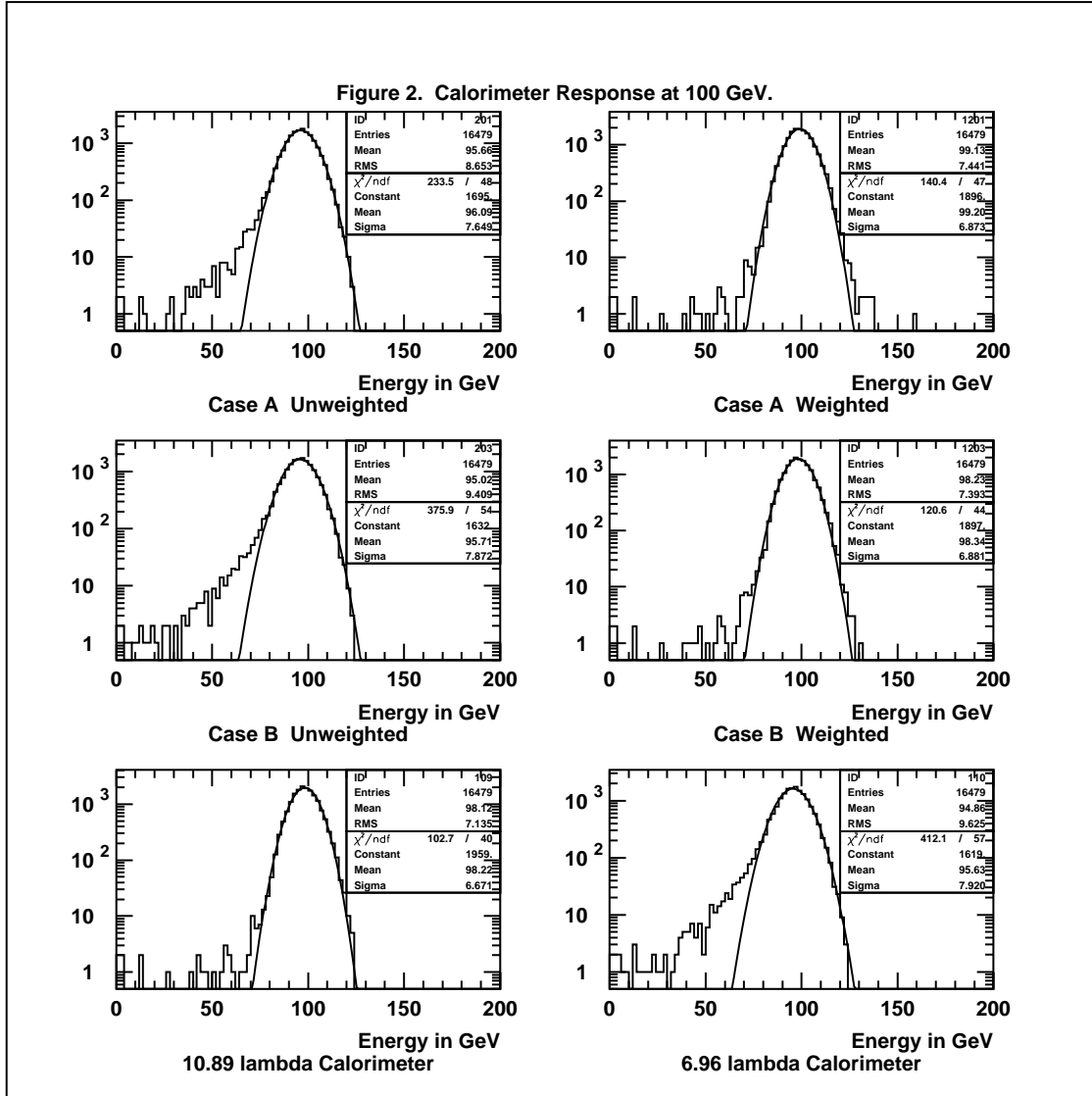


Figure 2. Calorimeter response for a 100 GeV π beam.

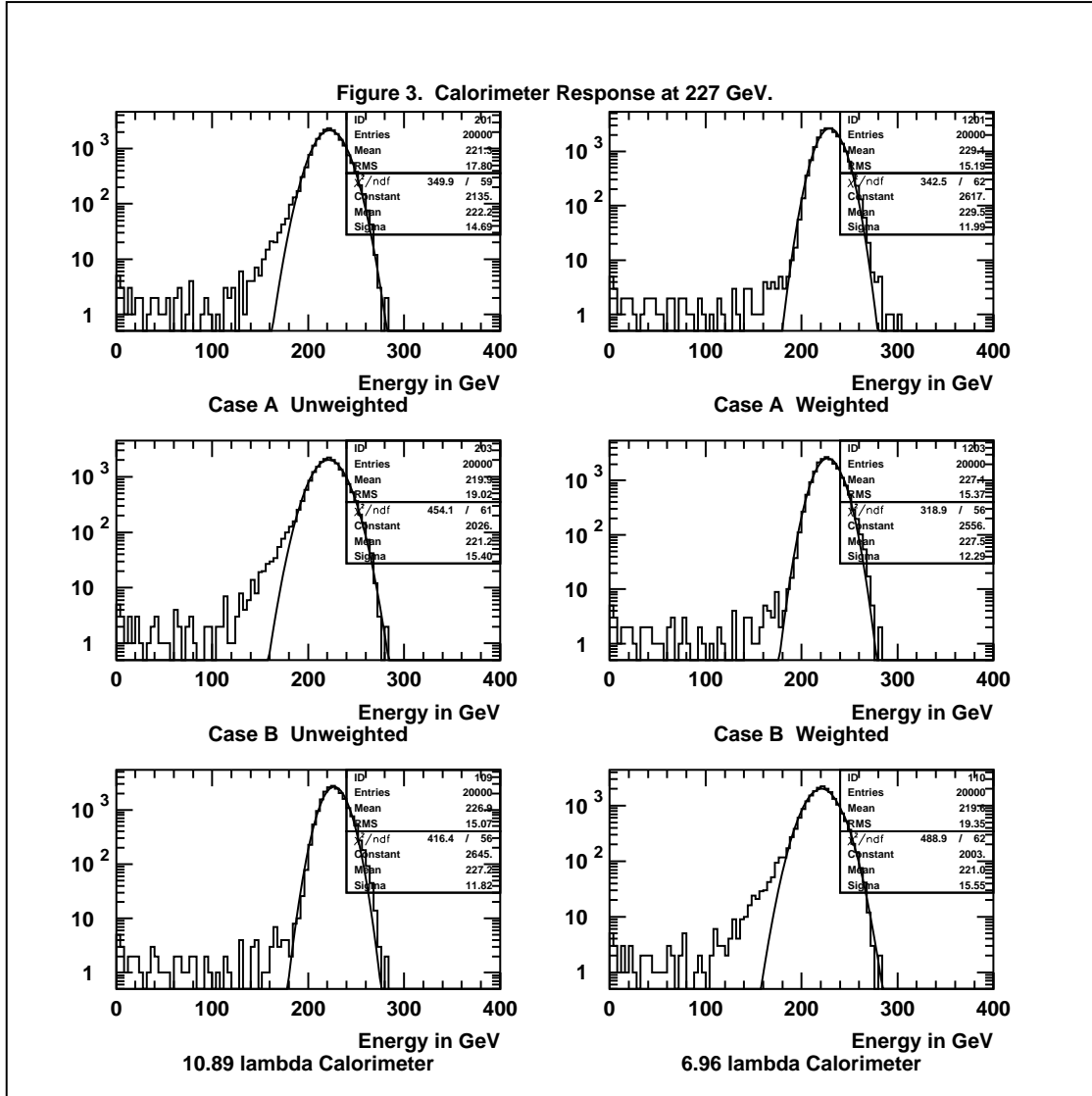


Figure 3. Calorimeter response for a 227 GeV π beam.

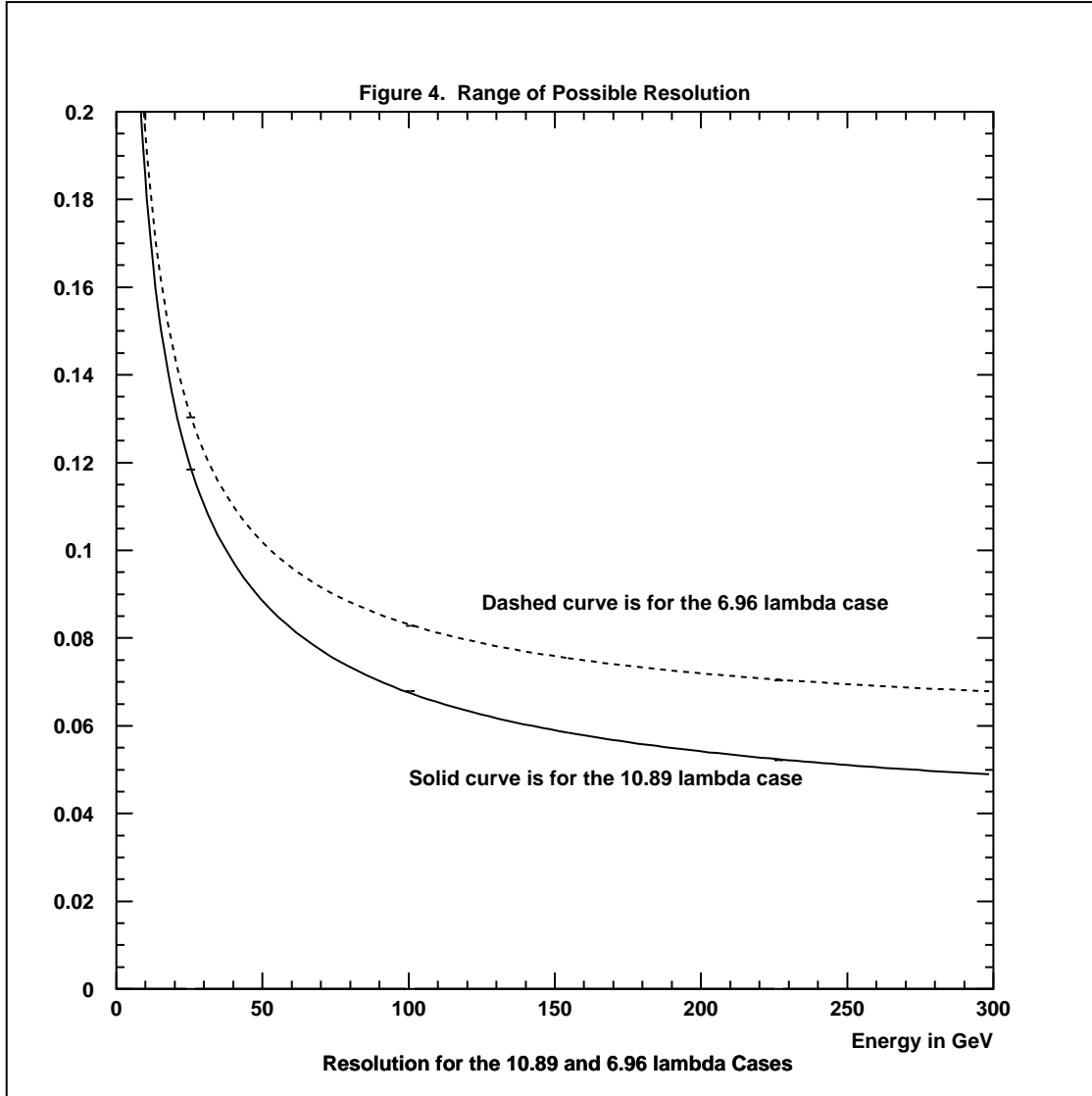


Figure 4. Calorimeter resolution as a function of beam energy. The solid curve corresponds to a 10.89λ depth and the dashed curve corresponds to a 6.96λ depth.

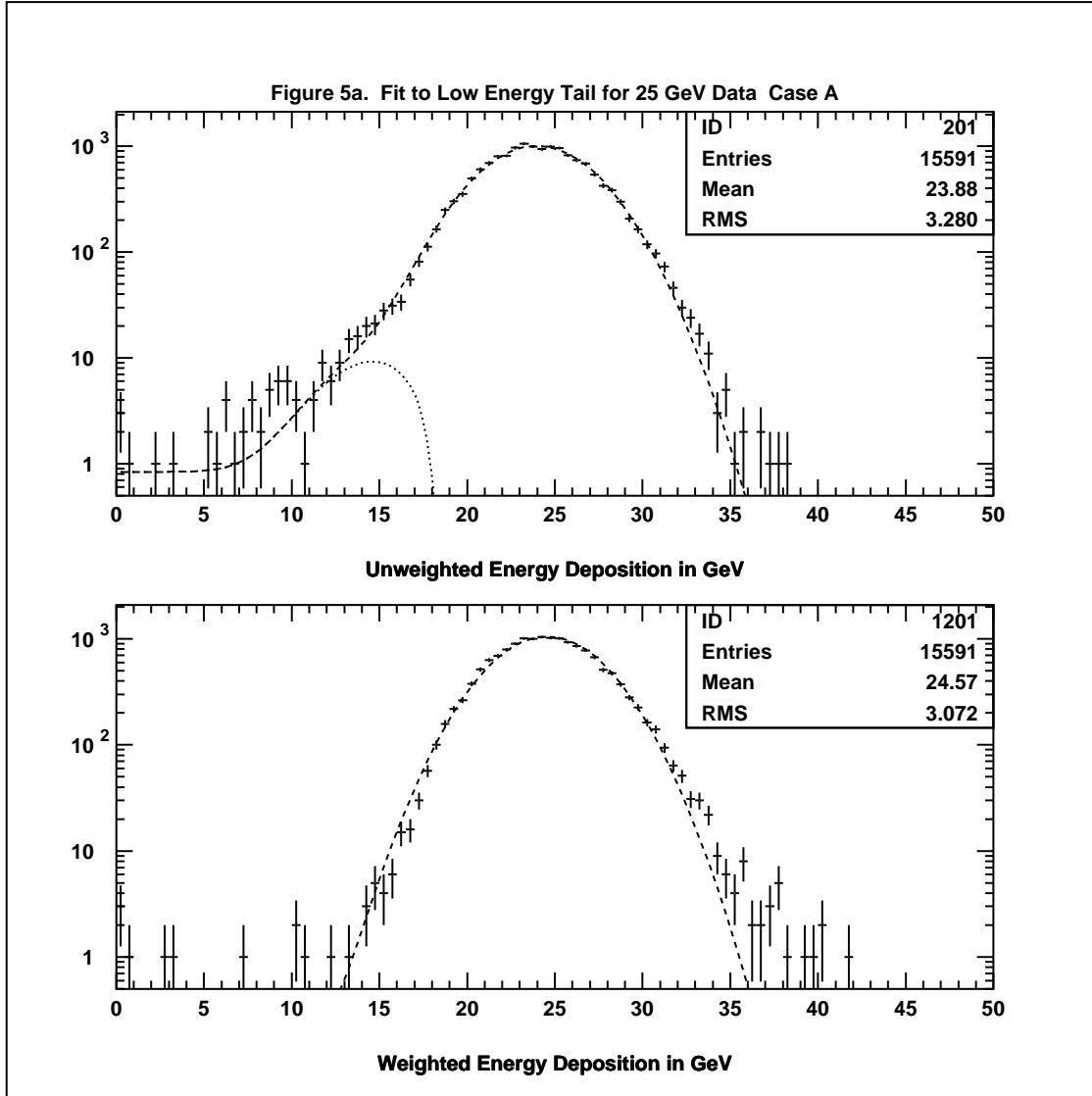


Figure 5a. Raw and weighted energy deposit distribution for a 25 GeV beam for Case A. The dashed curve shows the full fit while the dotted curve shows the fit to the low energy tail.

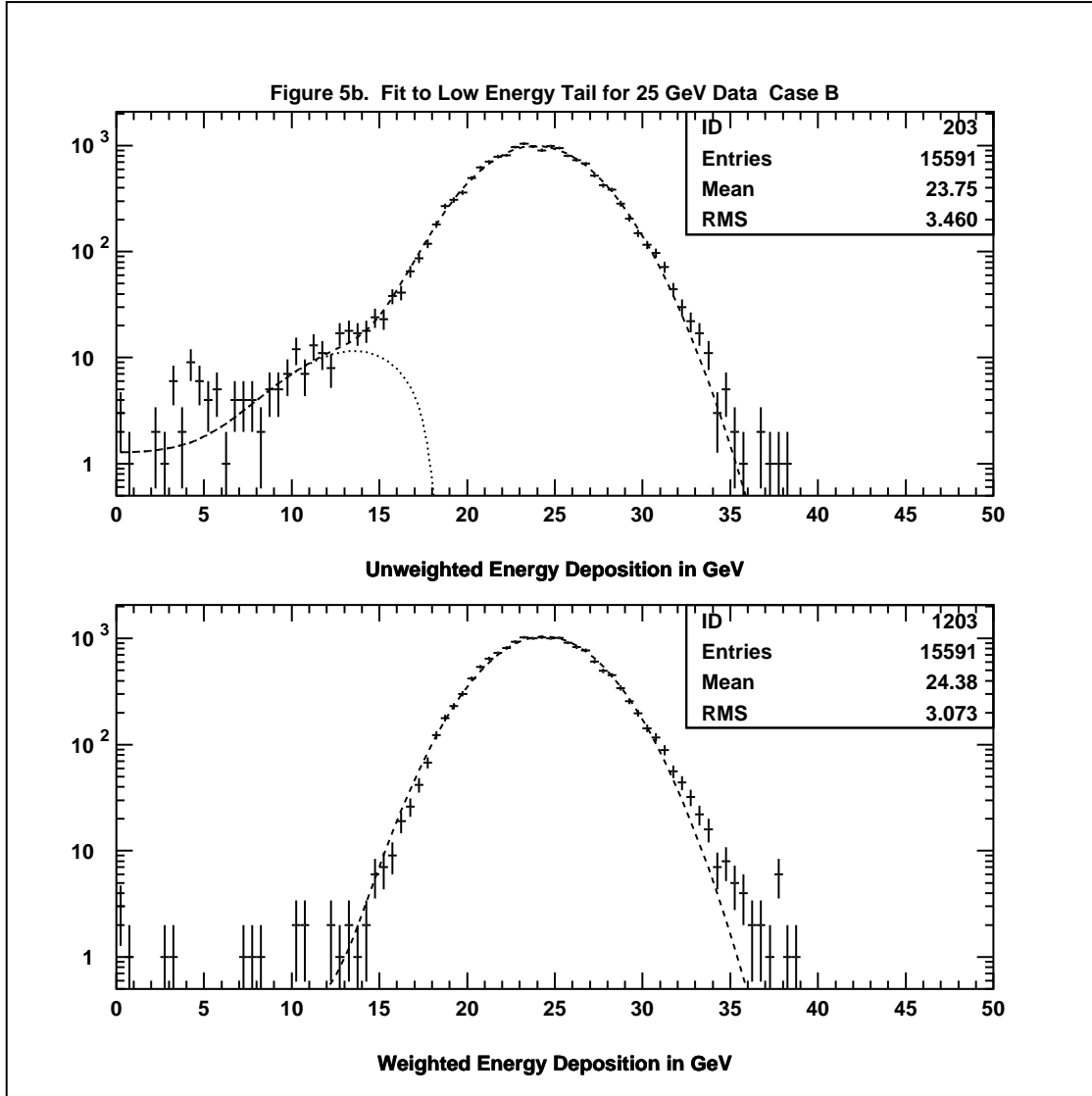


Figure 5b. Raw and weighted energy deposit distribution for a 25 GeV beam for Case B. The dashed curve shows the full fit while the dotted curve shows the fit to the low energy tail.

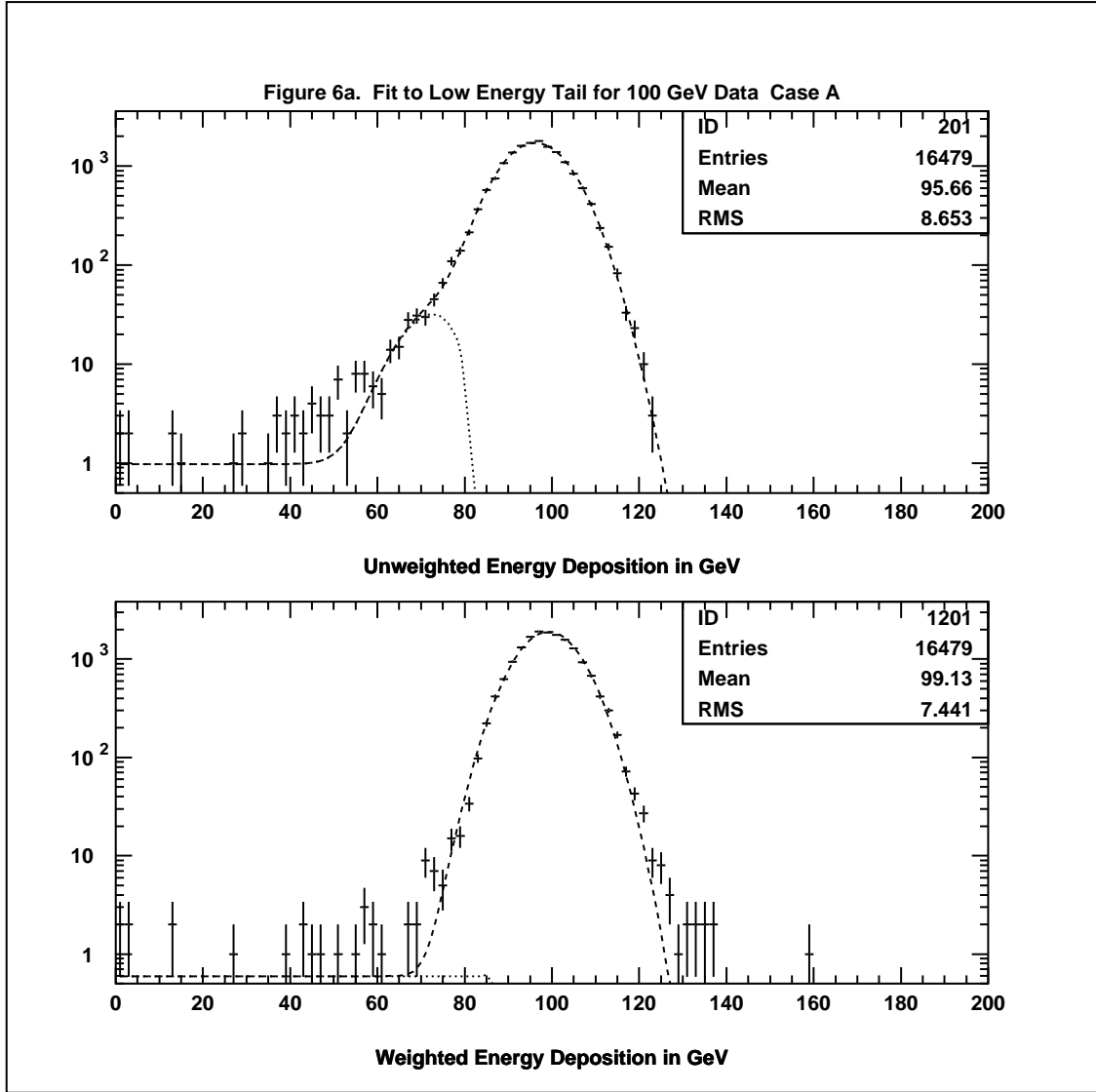


Figure 6a. Raw and weighted energy deposit distribution for a 100 GeV beam for Case A. The dashed curve shows the full fit while the dotted curve shows the fit to the low energy tail.

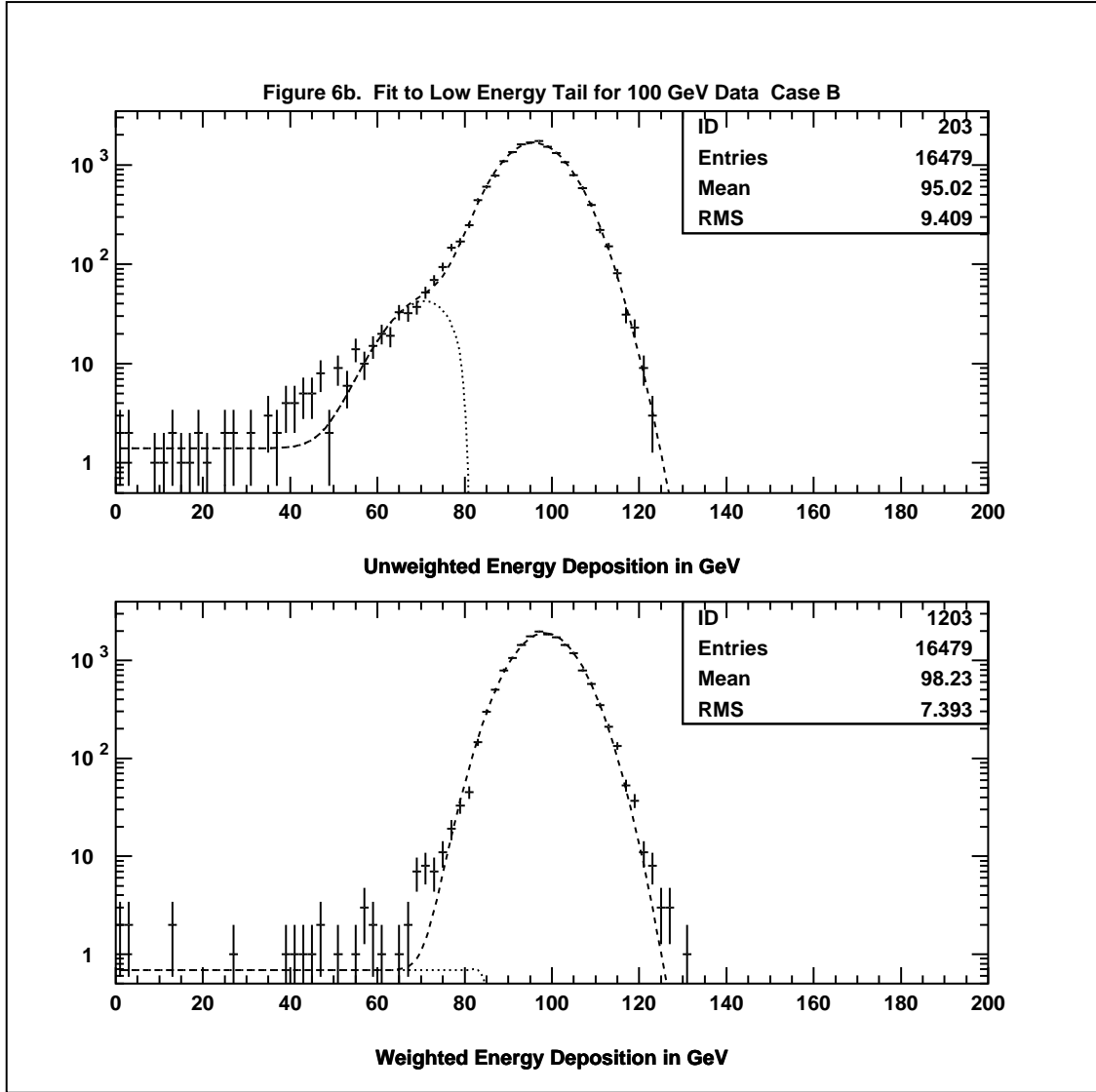


Figure 6b. Raw and weighted energy deposit distribution for a 100 GeV beam for Case B. The dashed curve shows the full fit while the dotted curve shows the fit to the low energy tail.

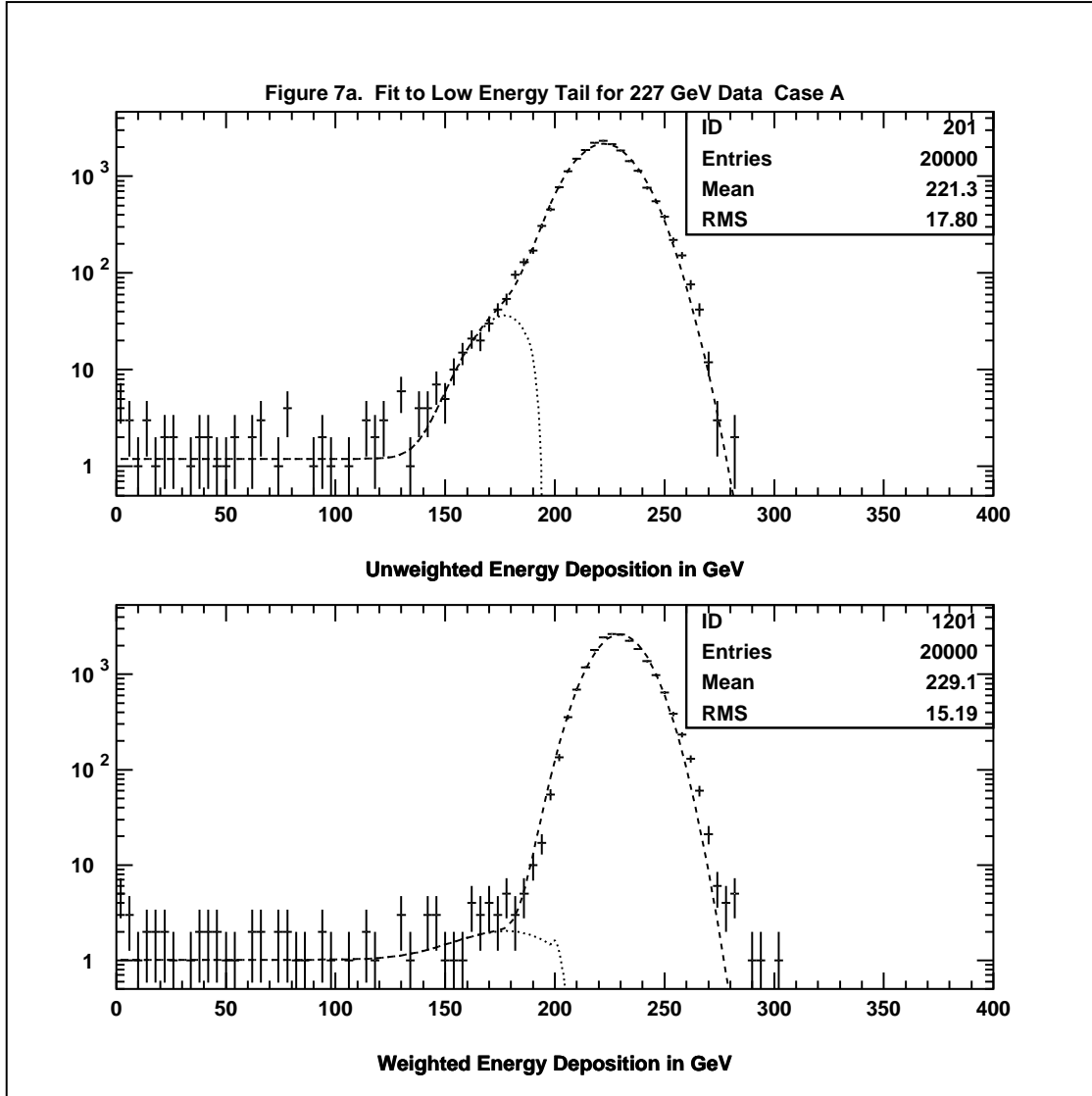


Figure 7a. Raw and weighted energy deposit distribution for a 227 GeV beam for Case A. The dashed curve shows the full fit while the dotted curve shows the fit to the low energy tail.

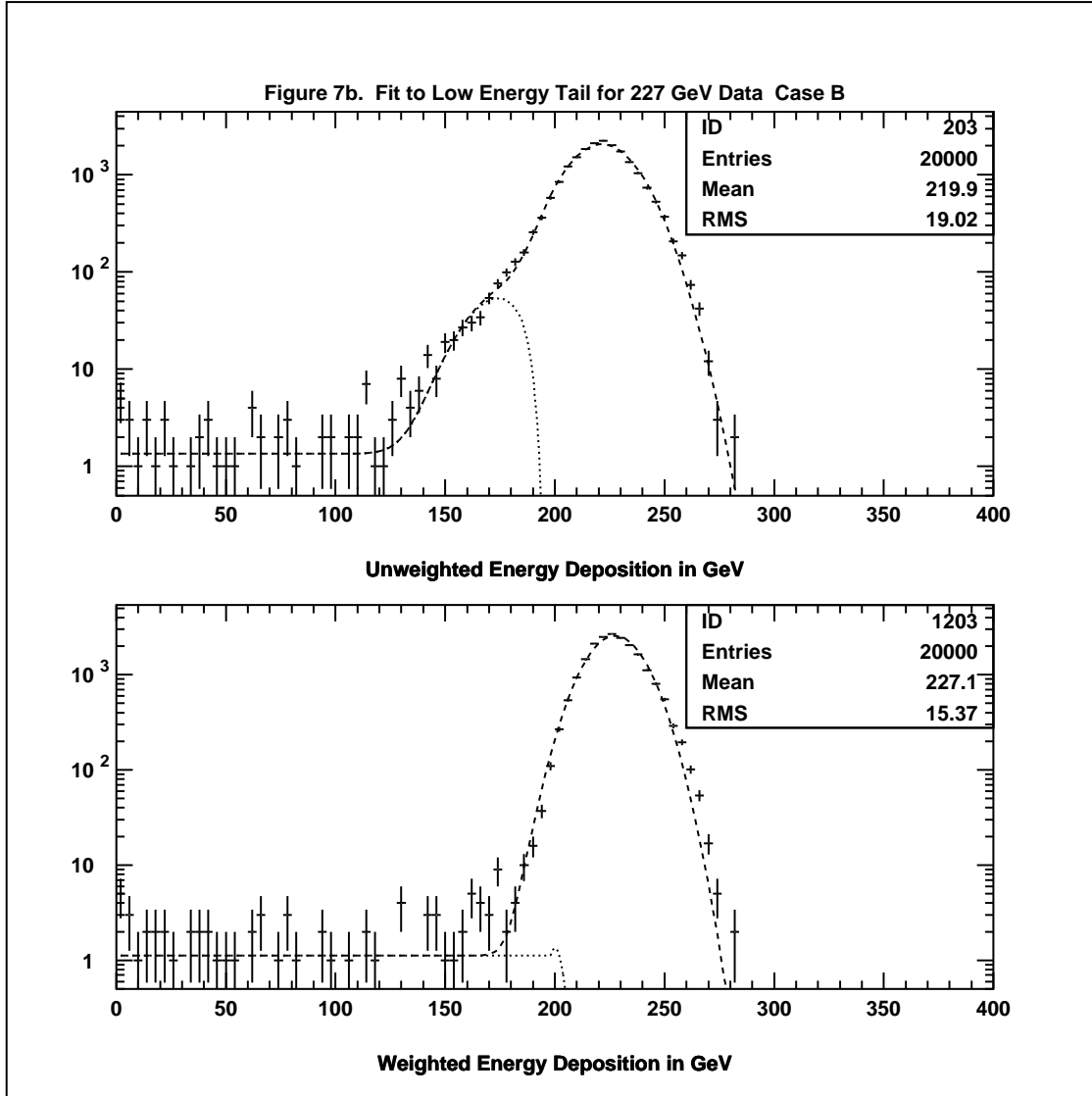


Figure 7b. Raw and weighted energy deposit distribution for a 227 GeV beam for Case B. The dashed curve shows the full fit while the dotted curve shows the fit to the low energy tail.

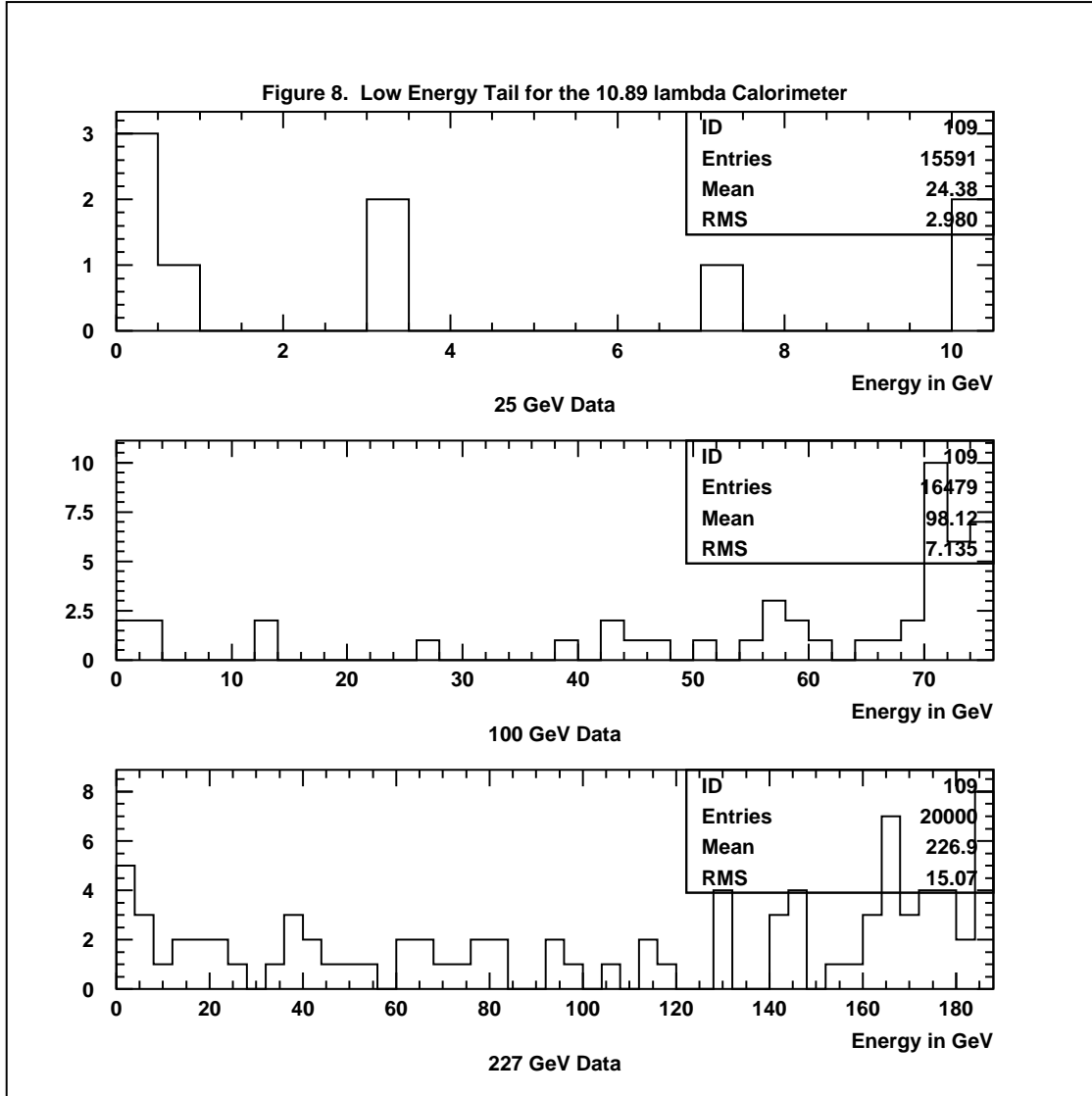


Figure 8. Unweighted low energy tail distribution for a 10.9λ calorimeter in response to 25 GeV, 100 GeV and 227 GeV π beams.

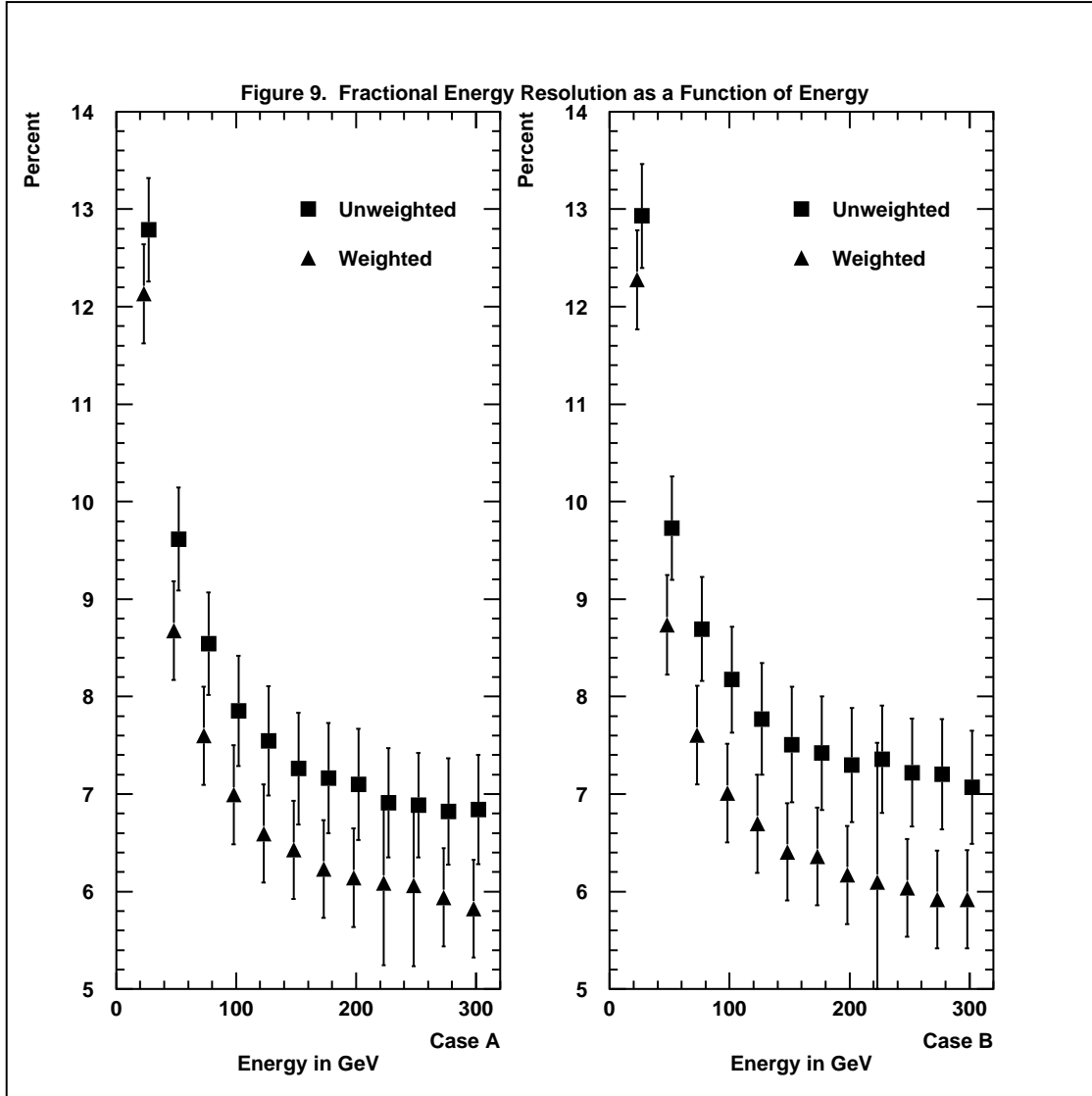


Figure 9. Comparison of the fractional energy resolution with and without a tail catcher.